





## Molecular Docking Screening and Pharmacokinetic Studies of Some Boron-Pleuromutilin Analogues against Possible Targets of *Wolbachia pipientis*

Fabian Audu Ugbe\* Gideon Adamu Shallangwa Adamu Uzairu Ibrahim Abdulkadir 

Department of Chemistry, Ahmadu Bello University, Zaria, Kaduna State, Nigeria

\*email: [ugbefabianaudu@gmail.com](mailto:ugbefabianaudu@gmail.com)

### Keywords:

Filarial diseases  
Molecular docking  
Pharmacokinetics  
Pleuromutilins  
*Wolbachia*

### Abstract

Lymphatic filariasis and onchocerciasis are two common filarial diseases caused by a group of parasitic nematodes called filarial worms, which co-habit with the bacteria organism *Wolbachia*. One good treatment approach seeks *Wolbachia* as a drug target. Here, a computer-aided molecular docking screening was conducted on a series of 52 pleuromutilin analogs against four *Wolbachia* enzymes:  $\alpha$ -DsbA1 (PDB: 3F4R),  $\alpha$ -DsbA2 (6EEZ), OTU deubiquitinase (6W9O), and cytoplasmic incompatibility factor CidA (7ESX) to find a more potent drug candidate(s) for the treatment of filarial diseases. The docking investigation was performed using the iGEMDOCK tool, while NAMD was utilized for the Molecular Dynamic (MD) simulation. The results of the virtual screening identified four ligand-protein interaction pairs with the highest binding affinities in the order: **17\_6W9O** (-117.31 kcal/mol) > **28\_6EEZ** (-104.43 kcal/mol) > **17\_7ESX** (-102.56 kcal/mol) > **41\_7ESX** (-101.51 kcal/mol), greater than that of the reference drug doxycycline\_7ESX (-92.15 kcal/mol). These molecules (**17**, **28**, and **41**) showed excellent binding interactions, making very close contact with the receptors' amino acid residues. They also showed better pharmacokinetic properties than doxycycline because they showed high intestinal absorption, were orally bioavailable and showed no AMES toxicity. Also, the stability of **17\_6W9O** interactions was confirmed by the MD simulation. Therefore, the selected molecules could be developed as potential drug candidates for treating filarial diseases.

Received: April 4<sup>th</sup>, 2022

Revised: June 23<sup>rd</sup>, 2022

Accepted: June 24<sup>th</sup>, 2022

Published: June 30<sup>th</sup>, 2022



© 2022 Fabian Audu Ugbe, Gideon Adamu Shallangwa, Adamu Uzairu, Ibrahim Abdulkadir. Published by Institute for Research and Community Services Universitas Muhammadiyah Palangkaraya. This is an Open Access article under the CC-BY-SA License (<http://creativecommons.org/licenses/by-sa/4.0/>). DOI: <https://doi.org/10.33084/jmd.v2i1.3450>

## INTRODUCTION

Lymphatic filariasis (LF), also known as elephantiasis and onchocerciasis (river blindness), are common Neglected Tropical Diseases (NTD), which are caused by some parasitic nematode worms<sup>1</sup>. LF is caused by filarial worms like *Wuchereria bancrofti*, *Brugia timori*, and *Brugia malayi*, transmitted by mosquitoes, while *Onchocerca volvulus* is the causative agent for onchocerciasis, which is transmitted from one person to another by blood-feeding blackflies<sup>2</sup>. Elephantiasis alone is responsible for not less than 2.8 million disabilities globally<sup>3</sup>.

The global program intended to eliminate these filarial diseases started far back through the Mass Drug Administration (MDA) of anti-filarial such as ivermectin, albendazole, and diethylcarbamazine, either as a dual (annual to bi-annual) or as triple-drug (once every three years) treatment<sup>3,4</sup>. However, it became unlikely that the MDA regimen will be adequate to eliminate these filarial diseases in all endemic areas, majorly due to their inability to kill

the macrofilarials<sup>5</sup>. Given the current scenario, therefore, a macrofilaricidal agent is required to kill adult worms to reduce both diseases' elimination time frames drastically<sup>6</sup>.

Fortunately, one unique characteristic of these filarial worms is their symbiotic co-existence with a known bacterium called *Wolbachia*<sup>7</sup>. In searching for new anti-filarial drugs, some researchers have chosen the option of targeting *Wolbachia*; past research showed that its elimination from the host filarial nematodes leads to antifilarial effects with the reduction of adult worm's lifespan<sup>8,9</sup>. Although the anti-bacteria drug doxycycline has been used clinically for treating filarial diseases over the years, the treatment method is not efficient enough for use in mass administration, including the requirement for extended treatment periods (4-6 weeks) as well as contraindications in pregnancy and children<sup>10</sup>. Therefore, advances in developing new anti-*Wolbachia* agents with short treatment periods and reduced complications are necessary.

Pleuromutilin was first reported in 1951 from the basidiomycetes *Pleurotus mutilis* (FR.) Sacc and *Pleurotus passeckerianus* Pilat<sup>11</sup>. Pleuromutilin and its analogs are antibacterial drugs that are inhibitors of protein synthesis in bacteria. Examples of antibiotics in this class include retapamulin, valnemulin, and tiamulin<sup>12</sup>. In the mid-1970s, much work was reported on using pleuromutilin analogs as veterinary antibiotics. Since then, several works have been undertaken to develop derivatives of the base structure for human use. Retapamulin became the first approved pleuromutilin antibiotic for human use, approved by the FDA in 2007<sup>13</sup>. Pleuromutilins have generally been reported to show potency against Gram-positive and some fastidious Gram-negative organisms<sup>14</sup>. Also, most pleuromutilins have an antibacterial spectrum covering the common pathogens involved in skin and respiratory tract infections<sup>15</sup>. This advantage has prompted the continuous exploration of compounds incorporating the pleuromutilin core as antibacterial agents. Jacobs *et al.*<sup>3</sup> were centered on synthesizing some boron-pleuromutilin derivatives as anti-*Wolbachia* agents with the potential for treating lymphatic filariasis and onchocerciasis. Some notable targets of *Wolbachia pipientis* include Oxidoreductase  $\alpha$ -DsbA1 (PDB ID: 3F4R), OTU deubiquitinase (6W9O), thiol-disulfide exchange protein  $\alpha$ -DsbA2 (6EEZ), and cytoplasmic incompatibility factor CidA (7ESX) amongst others.

Computer-aided drug design plays a crucial role in discovering new drug molecules in pharmaceutical design, drug metabolism, and medicinal chemistry. It saves time and cost and is highly effective for evaluating a sizeable virtual database of chemical compounds<sup>16</sup>. Molecular docking simulation is a computer-aided virtual screening method that probes the binding of ligands in the active sites of the protein target using a valid docking tool<sup>17</sup>. Pharmacokinetics analysis, on the other hand, is essential in the pre-clinical study of new drug compounds to ascertain how such drug compounds affect the living organism when administered. Some of the most critical pharmacokinetic properties to be determined during pre-clinical testing include absorption, distribution, metabolism, excretion, and toxicity (ADMET)<sup>18,19</sup>. Physico-chemical properties such as molecular weight (MW), topological polar surface area (TPSA), lipophilicity indices, hydrogen bond donors (HBD), and hydrogen bond acceptors (HBA), amongst others, are necessary to predict a drug's likelihood of being orally bioavailable<sup>20</sup>. Molecular dynamic (MD) simulation tends to probe the stability and rigidity of the protein-ligand interactions during a dynamically perturbed system<sup>21</sup>. This work focused on the *in-silico* molecular docking screening of a series of 52 boron-pleuromutilin derivatives against four *Wolbachia* targets, protein-ligand interaction study, prediction of pharmacokinetic properties, and MD simulation study of some selected analogs to find a more potent drug candidate(s) for the treatment of filarial diseases.

## MATERIALS AND METHODS

### Hardware and Software

The hardware used was an HP laptop computer with the following specifications: Processor (Intel® Core™ i5-4210U CPU @1.70GHz 2.40 GHz), Installed RAM (8.00 GB), System type (64-bit operating system, x64-based processor), Edition (Windows 10 Home Single Language), Version 21H2. Software used includes ChemDraw Ultra 12.0.2, Spartan '14 1.1.4 developed by Wave function Inc., Biovia Discovery Studio Visualizer 16.1.0.15350, iGEMDOCK (<http://gemdock.life.nctu.edu.tw/dock/>) made available online by the Drug Design and Systems Biology Laboratory of National Chiao Tung University, NAMD 2.14, and VMD 1.9.3 OpenGL Display. The online web servers; <http://www.swissadme.ch/index.php> and <http://biosig.unimelb.edu.au/pkcsdm> were used for the

pharmacokinetics properties prediction, while <https://www.charmm-gui.org> was used for generating ligand parameter files for molecular dynamics.

### Data Collection

A series of 52 Boron-pleuromutilin derivatives with reported biological activities ( $EC_{50}$ ) against *Wolbachia*-infected LDW1 cells (wMel) were obtained from the literature<sup>3</sup>. **Table I** shows the molecular structures of the various derivatives alongside their observed biological activities as obtained from the literature<sup>3</sup>. The  $pEC_{50}$  is the negative logarithm of  $EC_{50}$ .

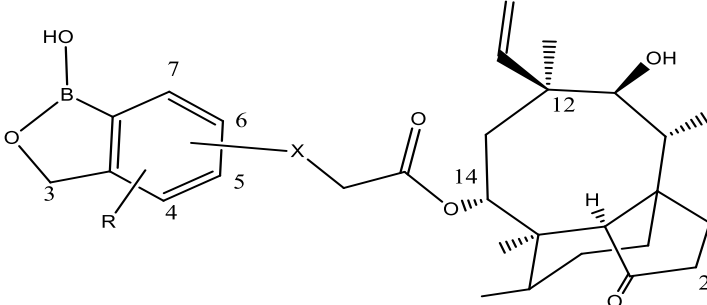
### Ligand Preparation

The two-dimensional structures of all the compounds, including the reference drug (doxycycline), were drawn with the help of ChemDraw Ultra 12.0.2, saved as MDL mol file format, and then fed separately into the Spartan 14 1.1.4 in three-dimensional (3D) structural form. The 3D structures were then optimized using Density Functional Theory (DFT) with Becke's three-parameter Lee-Yang-Parr hybrid (B3LYP) option and utilizing the 6-31G basis set. The thoroughly optimized structures were then saved in PDB file format for molecular docking study<sup>22,23</sup>. The molecular structure of doxycycline is shown in **Figure 1**.

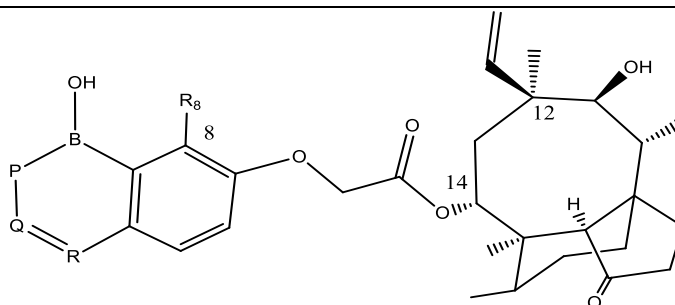
### Preparation of the Protein Receptors

The crystal structures of four *Wolbachia* receptors were obtained from the RCSB Protein Data Bank in PDB file format and then prepared separately using the Biovia Discovery Studio Visualizer by excluding water molecules and co-crystallized ligands enclosed within the protein structures<sup>24</sup>. The various receptors' chain A was utilized. The four receptors used in the virtual docking screening are described in **Table II**.

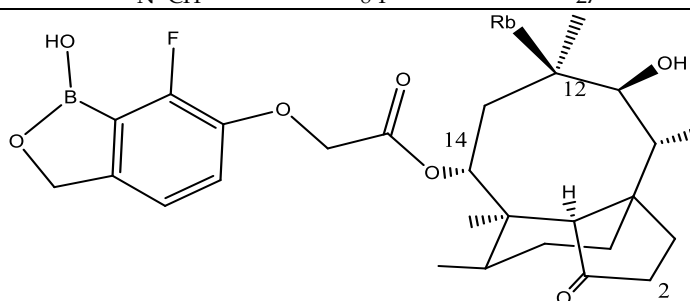
**Table I.** Molecular structures of pleuromutilin derivatives and their anti-*Wolbachia* activities



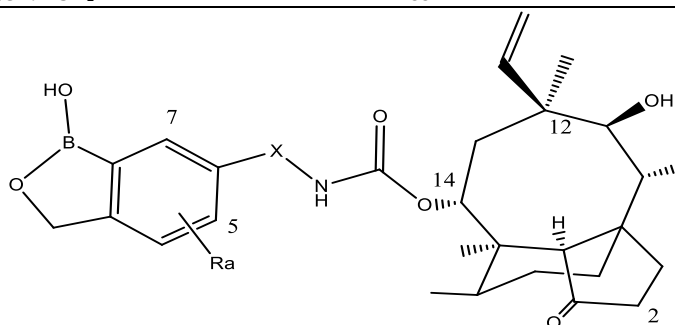
Compounds ID	Link atom	X	R	$EC_{50}$ (nM)	$pEC_{50}$
1 (pleuromutilin)	NA	OH	NA	6868	5.163359
2 (lefamulin)	NA	NA	NA	220	6.657577
3 (retapamulin)	NA	NA	NA	91	7.040959
4 (valnemulin)	NA	NA	NA	6.1	8.21467
5	6	O	5-Me	2.8	8.552842
6	6	O	7-Me	2.9	8.537602
7	6	O	7-F	1.5	8.823909
8	6	O	7-Cl	14	7.853872
9	6	O	7-OMe	3.7	8.431798
10	6	O	5,7-F <sub>2</sub>	1.2	8.920819
11	6	O	3-CH <sub>2</sub> NH <sub>2</sub>	19	7.721246
12	6	O	4-CH <sub>2</sub> NH <sub>2</sub>	18	7.744727
13	6	O	7-Cl, 3-CH <sub>2</sub> NH <sub>2</sub>	49	7.309804
14	6	O	7-F, 3-CH <sub>2</sub> NH <sub>2</sub>	317	6.498941
15	6	NH	3-CH <sub>2</sub> NH <sub>2</sub>	17	7.769551
16	6	NH	4-CH <sub>2</sub> NH <sub>2</sub>	44	7.356547
17	6	NH	7-CH <sub>2</sub> NH <sub>2</sub>	173	6.761954
18	6	NH	3,3-Me <sub>2</sub>	198	6.703335
19	6	NH	7-F	13	7.886057
20	6	S	H	17	7.769551
21	6	S	7-F	15	7.823909
22	6	-CH <sub>2</sub> NH <sub>2</sub> -	H	243	6.614394
23	6	-CH <sub>2</sub> NH <sub>2</sub> -	3,3-Me <sub>2</sub>	1418	5.848324
24	5	O	5-F	39	7.408935



	P	Q-R	Rs	EC <sub>50</sub> (nM)	pEC <sub>50</sub>
25	CH <sub>3</sub> SO <sub>2</sub> N	N=CH	H	0.8	9.09691
26	CH <sub>3</sub> N	N=CH	H	1.5	8.823909
27	CH <sub>3</sub> C(=O)N	N=CH	H	0.2	9.69897
28	Boc-N	N=CH	H	0.2	9.69897
29	HN	N=CH	H	2.7	8.568636
30	CH <sub>3</sub> OC(=O)N	N=CH	H	0.3	9.522879
31	O	N=CH	H	5.1	8.29243
32	CH <sub>3</sub> SO <sub>2</sub> N	N=CH	8-F	6.3	8.200659
33	CH <sub>3</sub> N	N=CH	8-F	11	7.958607
34	CH <sub>3</sub> OC(=O)N	N=CH	8-F	1.3	8.886057
35	O	N=CH	8-F	27	7.568636



	Rb	EC <sub>50</sub> (nM)	pEC <sub>50</sub>
36	Epoxide	13	7.886057
37	OHC-	33	7.481486
38	HOCH <sub>2</sub> -	242	6.616185
39	HON=CH-	71	7.148742
40	CH <sub>3</sub> ON=CH-	39	7.408935
41	Iso-C <sub>3</sub> H <sub>7</sub> ON=CH-	101	6.995679
42	CH <sub>3</sub> NHCH <sub>2</sub> -	1718	5.764977
43	C <sub>2</sub> H <sub>5</sub> NHCH <sub>2</sub> -	1399	5.854182
44	<i>n</i> -C <sub>3</sub> H <sub>7</sub> NHCH <sub>2</sub> -	478	6.320572
45	<i>n</i> -C <sub>4</sub> H <sub>9</sub> NHCH <sub>2</sub> -	243	6.614394
46	Cyclo-C <sub>3</sub> H <sub>7</sub> NHCH <sub>2</sub> -	44	7.356547
47	(CH <sub>3</sub> ) <sub>2</sub> NCH <sub>2</sub> -	439	6.357535
48	CH <sub>3</sub> ONHCH <sub>2</sub> -	133	6.876148



	X	Ra	EC <sub>50</sub> (nM)	pEC <sub>50</sub>
49	Bond	H	7.5	8.124939
50	Bond	5-F	14	7.853872
51	CH <sub>2</sub>	H	3.5	8.455932
52	CH <sub>2</sub>	7-F	4.9	8.309804

Note: NA-Not applicable; EC<sub>50</sub>: Half maximal effective concentration

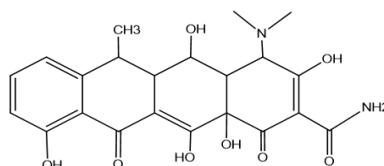


**Figure 1.** Molecular structure of the reference drug (doxycycline).

**Table II.** Description of enzymes used for the docking screening

No	Enzyme	Organism	PDB ID	Resolution (Å)
1	$\alpha$ -DsbA1	<i>Wolbachia</i>	3F4R	1.60
2	$\alpha$ -DsbA2	<i>Wolbachia</i>	6EEZ	2.25
3	OTU deubiquitinase	<i>Wolbachia</i>	6W9O	1.47
4	Cytoplasmic incompatibility factor CidA	<i>Wolbachia</i>	7ESX	1.80

### Virtual Docking Screening

Molecular docking investigation was conducted separately between the four different protein receptors of *W. pipientis* and all 52 compounds, as well as the reference drug (doxycycline) using the Generic Evolutionary Method for molecular docking (GEMDOCK) tool. GEMDOCK is a program for computing a ligand conformation and orientation relative to the target protein's active site. Here, the blind docking approach was adopted using the docking accuracy parameter settings for drug screening. This setting specified a population size of 200, a number of generations equal to 70, and a number of solutions equal to 3. GEMDOCK is an automatic system that generates all related docking variables, such as atom formal charge, atom type, and the ligand-binding site of a protein<sup>25</sup>. The best poses with the greatest negative values were then obtained and analyzed using iGEMDOCK's post-screening analysis tool and the Biovia Discovery Studio Visualizer, respectively<sup>26</sup>. This screening was carried out to identify the compounds that bind more strongly into the active pockets of the protein targets. iGEMDOCK calculates the binding energies of the protein-ligand (drug) interactions which are essential to describe how well the drug binds to the target macromolecule. The more negative the binding energy becomes, the greater the chances of the potential drug candidate initiating protein biochemical action/reaction<sup>27</sup>.

### Prediction of Pharmacokinetic Properties

Drug-likeness and ADMET properties prediction constitute a necessary stage in drug discovery's early phase because only molecules with good drug-likeness properties and excellent ADMET profiles advance into the pre-clinical research phase<sup>24</sup>. Hence, the three compounds with the best binding scores and the reference drug (doxycycline) were investigated for their pharmacokinetic properties using two online web servers, <http://www.swissadme.ch/index.php> for drug-likeness and <http://biosig.unimelb.edu.au/pkcsms> for ADMET profiling. The predicted parameters for drug-likeness include MW, TPSA, lipophilicity index (MlogP), HBD, HBA, and synthetic accessibility (SA) score. Some selected ADMET properties tested include human intestinal absorption (HIA), P-glycoprotein substrate/inhibitor, blood-brain barrier (BBB) permeability, central nervous system (CNS) permeability, CYP3A4 substrate/inhibitor, total clearance, and AMES toxicity. The choices of molecules for oral bioavailability have been guided by several rules such as Lipinski's 'rule of 5', Veber, Ghose, Egan, and Muegge rules<sup>28</sup>. Lipinski's RO5 is a widely used criterion for oral bioavailability. As such, these compounds would be assessed for oral bioavailability using the LRO5 criteria<sup>20</sup>.

### Molecular Dynamics Study

MD simulation of 17\_6W9O complex was performed using the combined approach of Chemistry at Harvard Macromolecular Mechanics (CHARMM) force field, Nano-scale Molecular Dynamics (NAMD), and Visual Molecular Dynamics (VMD). The CHARMM-GUI, an established web-based platform that utilizes the CHARMM force field, was used to generate the input files for the simulation by NAMD<sup>29</sup>. The periodic boundary condition was used while fitting the system into a cubic water box for solvation. The protein was solvated and neutralized explicitly in an aqueous solution of 0.1 M concentration of potassium chloride salt<sup>21</sup>. The simulation process involving energy minimization, equilibration (100 ps time frame), and production (500,000 steps or 1 ns time frame) was performed on the resulting system, while the results were visualized using VMD and the Biovia discovery studio<sup>30</sup>.

## RESULTS AND DISCUSSION

### Molecular Docking Study

The results (binding energies) of the docking simulation conducted between four protein receptors of *W. pipientis* and the boron-pleuromutilin compounds, as well as the reference drug (doxycycline), were reported in **Table III**, while the 3D representation of compound **17** in the active sites of the various receptors were shown in **Figure 2**.

**Table III.** Summary of interactions binding affinities of pleuromutilins and reference drug (doxycycline) with the different *W. pipientis* receptors used for the docking screening.

Compounds ID	Protein-ligand binding energies (kcal/mol)			
	3F4R	6EEZ	6W9O	7ESX
1 (pleuromutilin)	-77.10	-62.37	-76.71	-62.57
2 (lefamulin)	-71.43	-70.82	-71.88	-76.08
3 (retapamulin)	-74.49	-65.13	-70.88	-98.09
4 (valnemulin)	-77.53	-79.41	-69.64	-77.46
5	-80.71	-93.07	-74.31	-88.90
6	-76.06	-81.14	-76.74	-94.17
7	-81.59	-80.37	-89.81	-86.11
8	-78.51	-81.58	-89.83	-98.52
9	-71.13	-77.71	-80.13	-90.78
10	-80.85	-84.48	-84.94	-90.61
11	-92.11	-96.14	-82.47	-94.61
12	-78.38	-78.18	-83.33	-95.52
13	-79.99	-83.11	-84.26	-93.70
14	-82.26	-82.76	-79.57	-87.05
15	-78.78	-83.92	-82.21	-82.78
16	-75.59	-81.24	-76.63	-87.66
17	-75.41	-75.06	-117.31	-102.56
18	-86.03	-98.99	-94.27	-86.13
19	-85.72	-94.61	-82.37	-82.09
20	-94.88	-80.77	-92.59	-84.03
21	-77.38	-87.83	-79.10	-83.81
22	-90.60	-87.29	-88.24	-86.71
23	-90.83	-82.74	-88.42	-98.59
24	-72.89	-78.10	-81.28	-80.63
25	-89.47	-92.69	-83.99	-88.78
26	-81.01	-94.01	-80.46	-95.06
27	-81.39	-87.72	-77.66	-92.36
28	-80.85	-104.43	-86.62	-92.96
29	-91.67	-91.61	-87.47	-91.30
30	-92.13	-98.03	-90.72	-88.17
31	-77.17	-81.34	-91.48	-92.89
32	-82.51	-90.50	-90.67	-99.50
33	-76.14	-86.88	-80.53	-98.10
34	-82.71	-97.33	-84.40	-93.34
35	-79.56	-87.99	-81.65	-98.31
36	-80.97	-85.18	-78.47	-83.89
37	-83.60	-82.39	-81.33	-83.87
38	-92.79	-82.55	-80.00	-95.41
39	-88.59	-79.79	-87.40	-95.58
40	-81.03	-85.65	-77.25	-95.79
41	-77.78	-88.00	-76.22	-101.51
42	-77.90	-84.90	-78.82	-88.01
43	-85.05	-85.84	-86.98	-97.16
44	-77.88	-80.27	-90.00	-82.82
45	-89.71	-85.78	-81.43	-93.82
46	-92.64	-84.48	-79.03	-85.99
47	-80.21	-90.02	-78.91	-79.41
48	-81.82	-84.71	-84.81	-81.57
49	-84.69	-91.16	-90.98	-80.60
50	-80.71	-82.73	-88.76	-93.35
51	-85.71	-76.69	-82.02	-94.85
52	-81.89	-73.55	-82.91	-80.13
Doxycycline	-83.12	-89.34	-83.70	-92.15

Note: PDB ID – 3F4R, 6EEZ, 6W9O, 7ESX

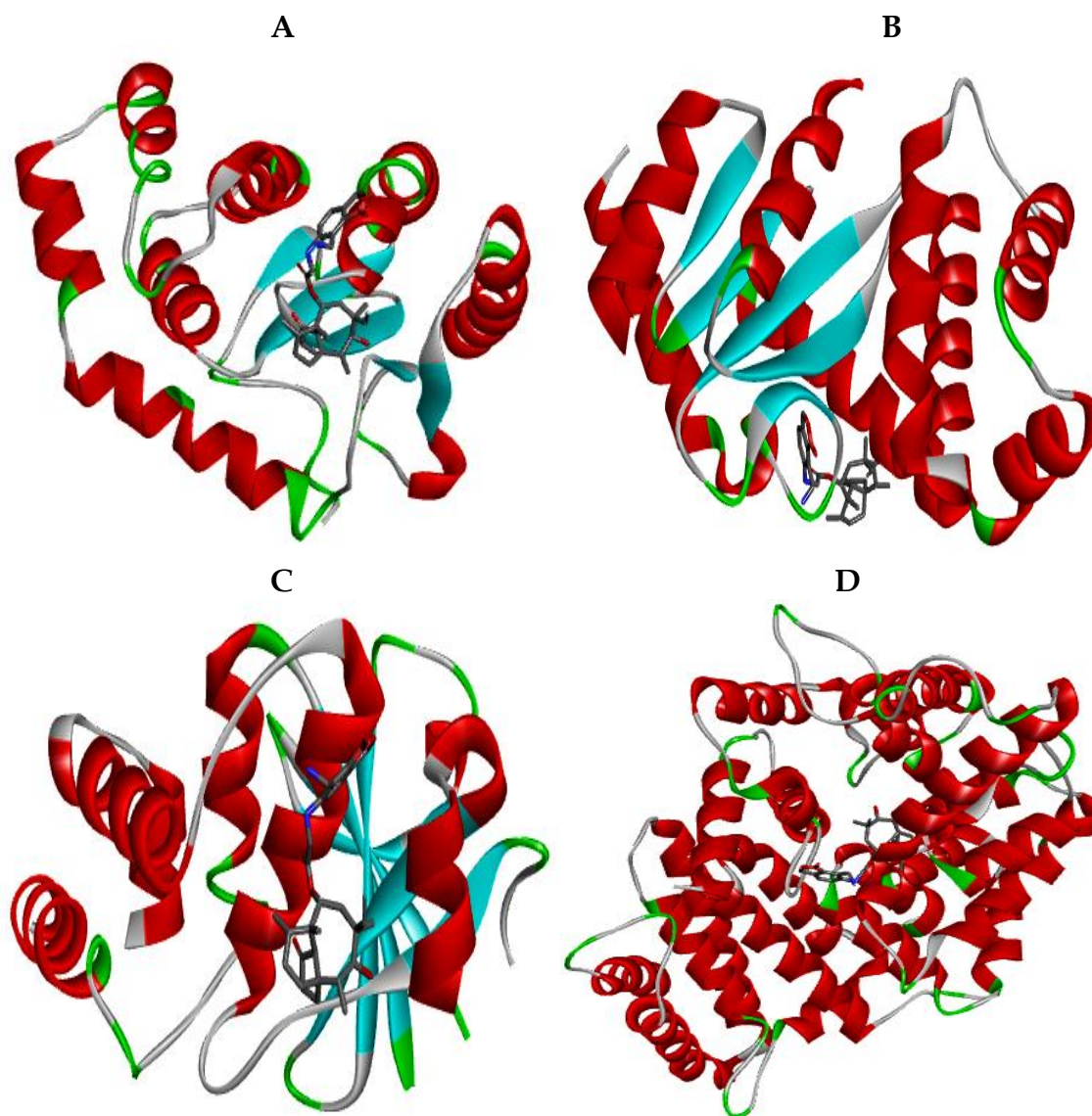


**Figure 2.** 3D representation of compound **17** in the active site of (A)  $\alpha$ -DsbA1 (PDB: 3F4R), (B)  $\alpha$ -DsbA2 (PDB: 6EEZ), (C) OTU deubiquitinase (PDB: 6W9O), and (D) cytoplasmic incompatibility factor CidA (PDB: 7ESX).

From the docking results, it can be shown that no particular receptor best interacts with all the studied compounds as a whole. A receptor may bind strongly with one compound but weakly interacts with another ligand. However, four ligand-protein interaction pairs with the greatest negative binding energies were identified in the order; compound **17**\_6W9O (-117.31 kcal/mol) > **28**\_6EEZ (-104.43 kcal/mol) > **17**\_7ESX (-102.56 kcal/mol) > **41**\_7ESX (-101.51 kcal/mol). Also, no ligand-protein pair involving the reference drug (doxycycline) and the clinically relevant pleuromutilins (compounds **1**, **2**, **3**, and **4**) could compare with the four identified ligand-protein pairs involving **17**, **28**, and **41**. Hence, subsequent discussion shall be based on these molecules. The reported experimental activities ( $pEC_{50}$ ) of the various pleuromutilin derivatives were shown in **Table I**, in which one of the selected compounds (**28**) possessed the highest  $pEC_{50}$  value of 9.6990. Also, compound **17** is more of a multi-target molecule, as evident in the high binding affinities with 6W9O and 7ESX. The pharmacological interactions between the receptors' amino acid residues and the selected compounds (**17**, **28**, and **41**), as well as the reference drug (doxycycline), were summarized in **Table IV**, while the 2D and 3D (hydrophobicity) views of the binding interactions as adapted from the Discovery Studio Visualizer were shown in **Figures 3 to 7**.

**Table IV.** Predicted binding interaction profiles of selected pleuromutilin derivatives and the reference drug (doxycycline) with some *W. pipientis* enzymes.

Complex	Binding energy (kcal/mol)	Hydrogen bond interactions			Electrostatic/hydrophobic interactions
		Amino acid	Type	Distance (Å)	
17_6W9O	-117.31	ARG-59	Conventional	2.08	GLU-63 ( $\pi$ -anion)
		ARG-59	Conventional	2.71	
		ARG-59	Conventional	2.78	
		GLN-46	Conventional	2.89	
		GLN-209	Conventional	2.51	
		GLU-63	Conventional	3.11	
17_7ESX	-102.56	GLU-47	Conventional	3.13	PHE-158 (alkyl), VAL-157 (alkyl), TRP-186 (alkyl), PHE-45 (alkyl), HIS-48 (alkyl), VAL-157 ( $\pi$ -alkyl), TRP-186 ( $\pi$ -alkyl), GLU-47 ( $\pi$ -anion)
		LYS-221	Conventional	1.77	
		LYS-221	Conventional	2.31	
		SER-104	Conventional	2.96	
		ASP-43	Carbon-hydrogen	2.95	
		PHE-45	$\pi$ -donor	3.80	
28_6EEZ	-104.43	-	-	-	LYS-72 (alkyl), LYS-72 ( $\pi$ -alkyl), LYS-242 (alkyl), VAL-239 (alkyl), PHE-231 (alkyl), ASP-228 ( $\pi$ -anion), ASP-68 ( $\pi$ -anion)
41_7ESX	-101.51	ASN-44	Conventional	2.85	PHE-45 (alkyl), HIS-48 (alkyl), PHE-158 (alkyl), TRP-186 (alkyl), VAL-157 (alkyl), TRP-186 ( $\pi$ -alkyl), VAL-157 ( $\pi$ -alkyl)
		GLU-47	Conventional	3.26	
		HIS-48	Conventional	3.17	
		LYS-221	Conventional	2.28	
Doxycycline_7ESX	-92.15	ASP-293	Conventional	2.92	-
		LYS-248	Conventional	1.65, 2.36	
		LYS-246	Conventional	2.62	
		SER-290	Conventional	3.10	
		VAL-250	Conventional	2.24	
		TYR-251	Conventional	2.20	
		LYS-248	Carbon-hydrogen	3.70	
ASP-247	Carbon-hydrogen	3.35			

As seen from **Table IV**, compound **17** was observed to have interacted well with the binding site of the OTU deubiquitinase receptor through six conventional hydrogen bonds (H-bonds) and two electrostatic interactions of the  $\pi$ -anion type. Five of the H-bonds were formed between carbonyl and hydroxyl groups of the pleuromutilin core and ARG-59 (at distances of 2.08, 2.71, and 2.78 Å), GLN-46 at a distance of 2.89 Å, and GLN-209 at a distance of 2.51 Å, while one H-bond was formed between the amino group on the benzoxaborole group and GLU-63 at a distance of 3.11 Å. The two  $\pi$ -anions were between GLU-63 and each of the  $\pi$ -electron systems of the five and six-membered rings on the benzoxaborole group. No hydrophobic interaction was identified, as shown in **Figure 3**.

The binding interaction profile of **17** with the binding site of cytoplasmic incompatibility factor CidA shows a fair combination of H-bonding and hydrophobic interactions, including electrostatic interactions. These include four conventional H-bonds with GLU-47 at a bond distance of 3.13 Å, LYS-221 (distance of 1.77 Å and 2.31 Å), and SER-104 at a distance of 2.96 Å. Also formed was a carbon-hydrogen bond with ASP-43 at a distance of 2.95 Å and  $\pi$ -donor hydrogen bonding with PHE-45 at a bond distance of 3.80 Å. Others include hydrophobic interactions majorly of the alkyl and  $\pi$ -alkyl interaction types, and electrostatic interactions of the  $\pi$ -anion type with GLU-47 at distances of 4.75 Å and 4.84 Å. The 3D view of the interaction between **17** and CidA in **Figure 4** confirmed that **17\_7ESX** interactions showed more hydrophobicity than **17\_6W9O**.

The binding interaction of **28** with  $\alpha$ -DsbA2 (PDB: 6EEZ) binding pocket showed no H-bond interaction but was dominated by alkyl and  $\pi$ -alkyl hydrophobic interactions, and  $\pi$ -anion electrostatic interactions with ASP-228 and ASP-68 at bond distances of 4.54 Å and 3.87 Å respectively. **Figure 5** shows the high hydrophobicity of **28\_6EEZ** interactions. A Similar result was obtained elsewhere<sup>24</sup>.

The binding interaction profile of **41** with CidA (PDB: 7ESX) showed four conventional H-bonds with ASN-44, GLU-47, HIS-48, and LYS-221 at bond distances of 2.85, 3.26, 3.17, and 2.28 Å respectively. Others include six alkyl and two  $\pi$ -alkyl hydrophobic interactions. The 2D and 3D views of the **41\_7ESX** interaction profile are shown in **Figure 6**.

Seven conventional H-bonds and two carbon-hydrogen bonds were identified for the binding interaction profile of doxycycline with CidA. These include conventional H-bonds with ASP-293 at a distance of 2.92 Å, LYS-246 at 2.62 Å, SER-290 at 3.10 Å, LYS-248 at 1.65 Å and 2.36 Å, VAL-250 at 2.24 Å, and TYR-251 at a distance of 2.20 Å. The carbon-



hydrogen bonds include LYS-248 at a distance of 3.70 Å and ASP-247 at a bond distance of 3.35 Å. No hydrophobic and electrostatic interactions were formed. The hydrophobicity surface of the doxycycline\_7ESX complex is shown in **Figure 7**.

Hence, these compounds (**17**, **28**, and **41**) have demonstrated adequate binding interactions with the studied target enzymes and represent potent *Wolbachia* inhibitors. The binding affinities of the four clinically relevant pleuromutilins: pleuromutilin, lefamulin, retapamulin, and valnemulin with the various enzymes of *W. pipientis* were less intense compared to those of the boron-pleuromutilin analogs as observed from **Table III**. From the pharmacological interaction profiles in **Figures 3** to **7**, it was observed that incorporating the benzoxaborole group into the pleuromutilin structure greatly improved the interactions of the boron-pleuromutilin analogs with the various target receptors, therefore leading to high binding affinities.

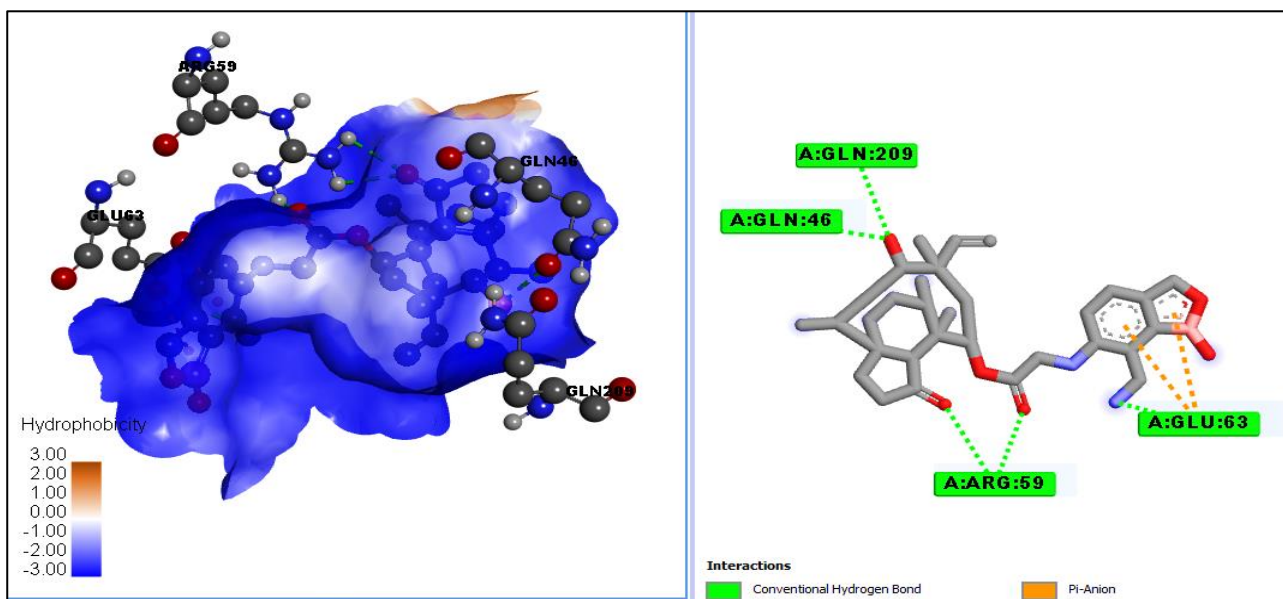


**Figure 3.** 3D (left) and 2D (right) view of the interaction between **17** and OTU deubiquitinase.

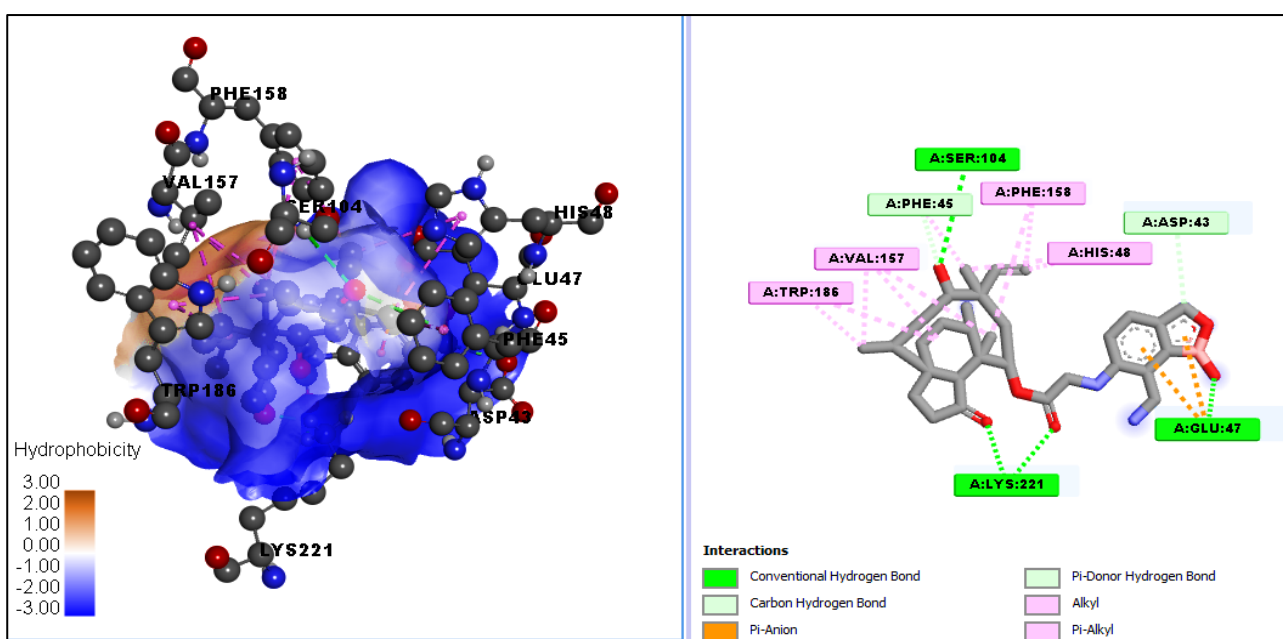


**Figure 4.** 3D (left) and 2D (right) view of the interaction between **17** and CidA.

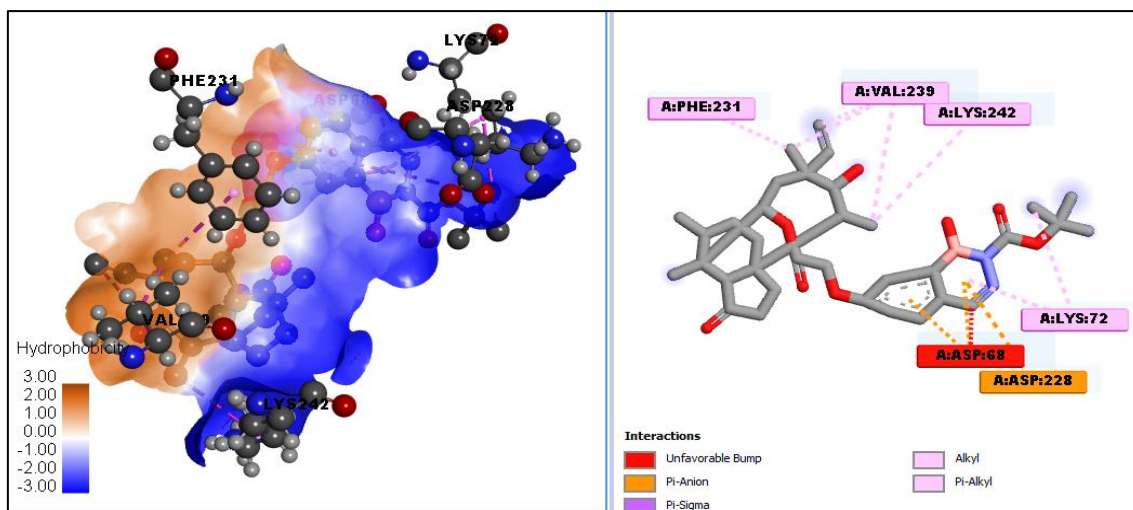


Figure 5. 3D (left) and 2D (right) view of the interaction between 28 and  $\alpha$ -DsbA2 receptor.

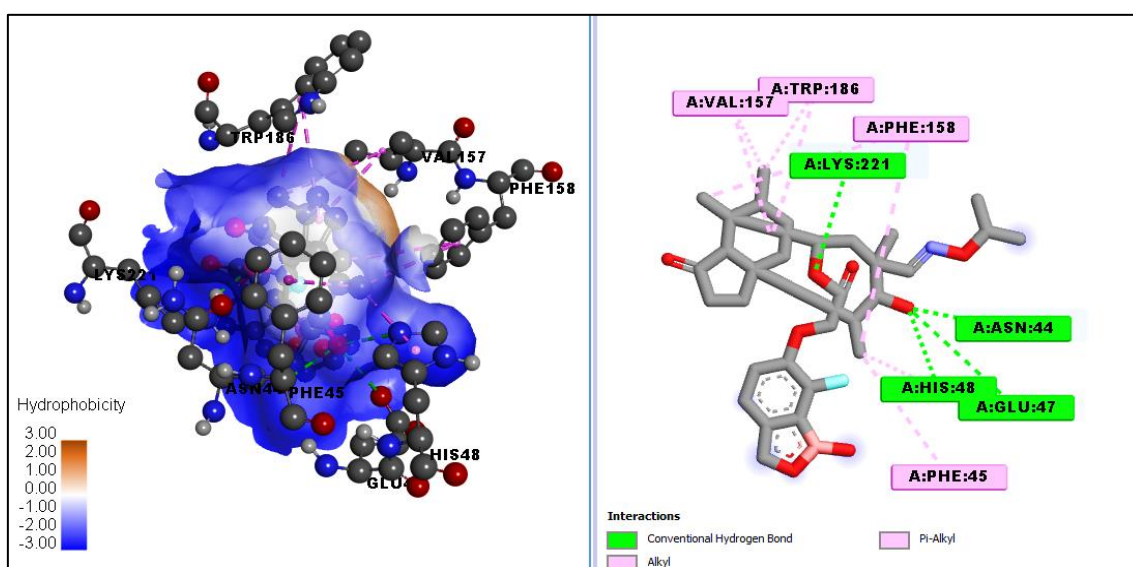


Figure 6. 3D (left) and 2D (right) view of the interaction between 41 and CidA.

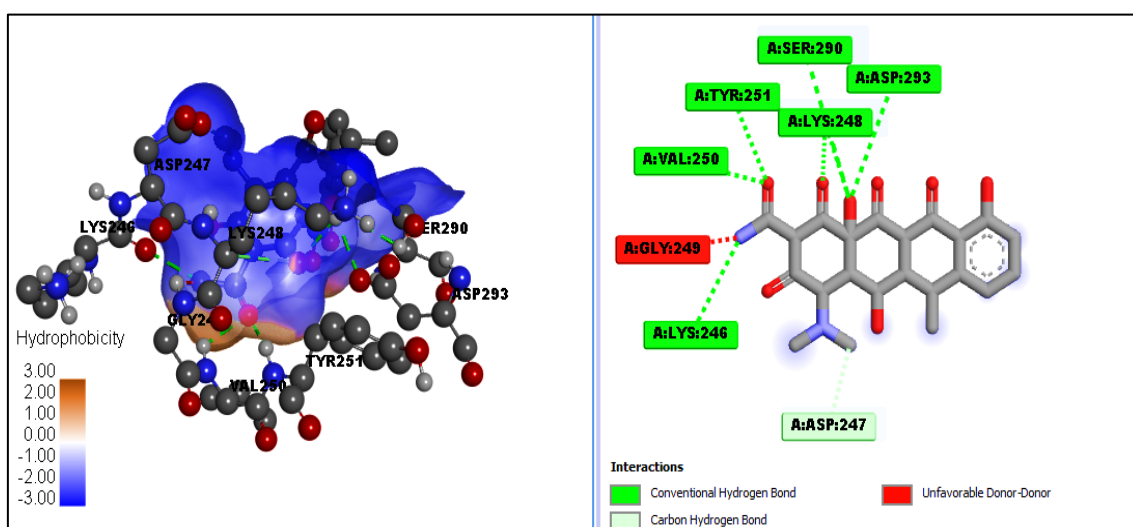


Figure 7. 3D (left) and 2D (right) view of the interaction between doxycycline and CidA.

### Pharmacokinetic Properties

Drug-likeness analysis and ADMET study were conducted on the four compounds (**17**, **28**, **41**, and doxycycline) to ascertain their oral bioavailability and drug-likeness attributes. The results of both investigations are presented in **Tables V** and **VI**. Lipinski's rule for oral-bioavailability states that a drug molecule is more likely to have poor absorption or permeation when it has an HBD of greater than 5, HBA > 10, MW > 500, and lipophilicity index (MLOGP > 4.15 or WLOGP > 5)<sup>20</sup>. Usually, molecules that obey at least three of the four requirements are said to be orally bioavailable<sup>18</sup>. **Table V** shows that all the molecules obeyed Lipinski's RO5 since they satisfied at least three of the four requirements. The only violation resulted from the molecules having MW of greater than 500 for the selected pleuromutilins, while doxycycline showed an HBD greater than 5. Also, the reported values of TPSA for the selected pleuromutilin molecules were less than the threshold value of 140 Å<sup>2</sup>, beyond which a molecule may exhibit poor HIA. On the other hand, doxycycline showed a TPSA of 181.62 Å<sup>2</sup> (well above the threshold). The SA scores are in the order of doxycycline < **17** < **41** < **28**, indicating fewer rigors in the laboratory synthesis of doxycycline compared to **17**, **41**, and **28** in that order. A similar observation was reported elsewhere<sup>26</sup>.

The predicted ADMET properties in **Table VI** showed good intestinal absorption of more than 75% for all the selected pleuromutilins, while doxycycline exhibited poor HIA, perhaps due to its high TPSA reported earlier. All the molecules presented were substrates of P-glycoprotein, which act as a biological barrier by extruding toxins and xenobiotics, including drugs, out of cells. Interestingly, the selected analogs were also inhibitors of both P-glycoprotein I and II, except **17**, which was predicted to inhibit P-glycoprotein I only, evidence that the molecules may be mediated well to reach their target sites without being isolated by the P-glycoprotein. This was not the case for doxycycline, as the prediction showed no inhibition of p-glycoprotein. Additionally, only **28** and **41** were substrates and inhibitors of the selected cytochrome P450 enzyme (CYP-3A4), an essential enzyme for drug metabolism in the body, which means a well-regulated (optimal) metabolic process for the molecules in the body.

Furthermore, all the molecules showed a logarithmic ratio of brain to plasma drug concentration (logBB) of less than 0.3, indicating they do not readily permeate through the BBB. Also, the molecules all showed poor CNS permeability since the blood-brain permeability-surface area product (logPS) values were less than -2. The total clearance for a drug molecule in the body for these molecules is within the accepted range, while they showed no AMES toxicity, indicating that the molecules are non-mutagenic and, as such non-carcinogenic. The results of the ADMET study compare very well with those of similar studies earlier reported<sup>24,26</sup>. Based on the predicted parameters, therefore, the selected molecules (**17**, **28**, and **41**) were said to possess relatively better pharmacokinetics profiles being that they; showed high intestinal absorption, conformed to Lipinski's RO5 for oral bio-availability, were substrates and inhibitors of P-glycoprotein, and showed no AMES toxicity.

**Table V.** Predicted drug-likeness properties of selected pleuromutilin derivatives and reference drug (doxycycline).

ID	MW (g/mol)	TPSA (Å <sup>2</sup> )	MLOGP	HBD	HBA	SA	LRO5 Violation	Drug-likeness
<b>17</b>	538.48	131.11	1.65	4	7	6.81	1	Yes
<b>28</b>	622.56	134.96	2.73	2	9	7.53	1	Yes
<b>41</b>	587.48	123.88	2.24	2	10	7.20	1	Yes
Ref	444.43	181.62	-2.08	6	9	5.15	1	Yes

Note: MW-molecular weight; TPSA-topological polar surface area; HBD-hydrogen bond donors; HBA-hydrogen bond acceptors; LRO5-Lipinski rule of five; SA-synthetic accessibility score; Ref-Reference drug (doxycycline).

**Table VI.** Predicted ADMET properties of selected pleuromutilin derivatives and reference drug (doxycycline).

ID	Absorption			Distribution		Metabolism		Excretion	Toxicity	
	HIA	P-glycoprotein			BBB	CNS	CYP-3A4		Total clearance	AMES toxicity
		S	I	II			logBB	logPS		
<b>17</b>	77.965	Yes	Yes	No	-0.910	-3.155	No	No	0.560	No
<b>28</b>	92.136	Yes	Yes	Yes	-1.157	-2.746	Yes	Yes	-0.091	No
<b>41</b>	94.208	Yes	Yes	Yes	-0.713	-3.218	Yes	Yes	0.126	No
Ref	31.193	Yes	No	No	-1.763	-3.829	No	No	0.241	No

Note: BBB-Blood brain barrier; CNS-Central nervous system; HIA-Human intestinal absorption; logBB-logarithmic ratio of brain to plasma drug concentration; logPS-blood-brain permeability-surface area product; CYP-3A4-cytochrome p450 isoform; S-substrate; I-inhibitor; II-inhibitor II; Ref-Reference drug (doxycycline).

### Molecular Dynamic Study

To ascertain the stability and rigidity of the protein-ligand interactions, 17\_6W9O, with the highest binding score, was subjected to MD simulation. The results of the simulation, summarized as plots of root-mean-square deviation (RMSD), root-mean-square fluctuation (RMSF), and solvent accessible surface area (SASA) versus the time in picoseconds (ps), were presented in Figure 8. From the RMSD plot in Figure 8A, it can be inferred that the complex became stable from 800 to 1000 ps during the simulation, indicating that the system was fast in attaining stability<sup>31</sup>. RMSF is more like a calculation of the flexibility or the extent of movement of individual residue during a simulation. As seen from Figure 8B, the RMSF tends to decrease slightly as the simulation nears 1000 ps, a further indication that the system was fast attaining stability. The SASA is the surface area in contact with the complex's solvent. Figure 8C shows that the SASA only fluctuates slightly between 8.50 Å<sup>2</sup> and 9.30 Å<sup>2</sup> during the trajectory, connoting stability<sup>21</sup>. Furthermore, the simulated complex was inspected for possible protein-ligand interactions. The resulting interactions (Figure 8D) deviated significantly from that of the non-simulated complex (Figure 3), as all of the conventional H-bonds were lost. However, a significant number of essential interactions were visible, including two C-H bonds with GLN-60 at interaction distances of 2.91 Å and 3.02 Å, two  $\pi$ -anion interactions with GLU-63, and a  $\pi$ -alkyl hydrophobic interaction with TYR-43. The two  $\pi$ -anion interactions with GLU-63 were common between the simulated and non-simulated complexes and perhaps played a very significant role in the stability of the complex, especially during the trajectory. Additionally, no unfavorable steric bumps or clashes were visible. It can therefore be inferred that compound 17 binds readily with OTU deubiquitinase even within a dynamically perturbed system.

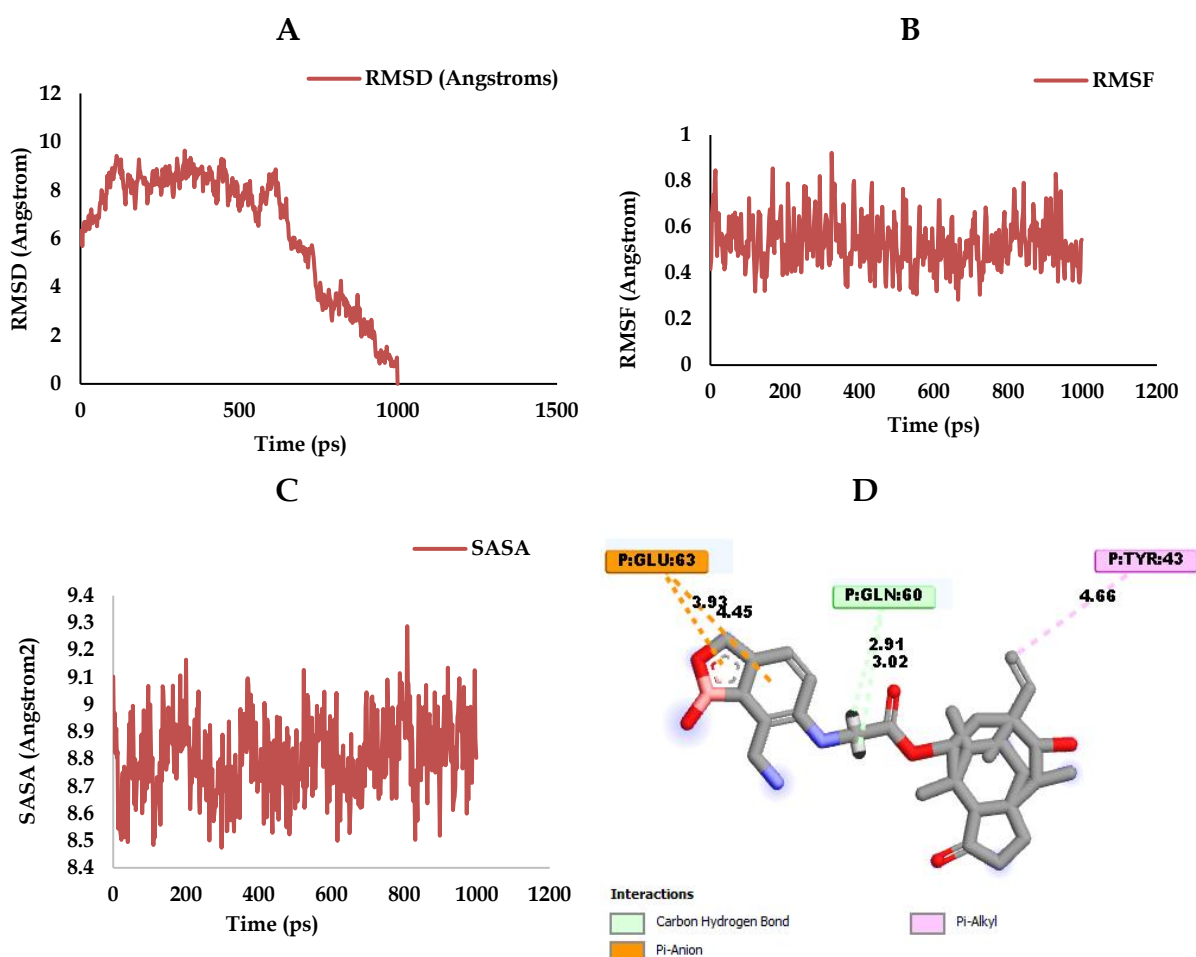


**Figure 8.** MD simulation study of compound 17 and OTU deubiquitinase complex (17\_6W9O). (A) Plot of RMSD versus time (ps), (B) Plot of RMSF versus time (ps), (C) plot of SASA versus time (ps), and (D) Protein-ligand binding interactions.

## CONCLUSION

The virtual docking screening identified three compounds (**17**, **28**, and **41**) as the most active molecules forming the more energetically stable complexes; **17\_6W9O**, **17\_7ESX**, **28\_6EEZ**, and **41\_7ESX**. These compounds predicted pharmacological interaction profiles generally fit well into the target site cavities. Also, these molecules were said to be orally bioavailable and showed better pharmacokinetic properties than the reference drug (doxycycline). Additionally, the MD simulation revealed the stability of **17\_6W9O** interactions. Hence, the selected molecules could be developed and further evaluated as potential drug candidates for the treatment of filarial diseases.

## ACKNOWLEDGMENT

The authors sincerely acknowledge G.F.S. Harrison Quantum Chemistry Research Group, Ahmadu Bello University Zaria, for providing all software and suitable environment utilized for this study.

## CONFLICT OF INTEREST

The authors declared that there are no conflicts of interest.

## FUNDING

None.

## DATA AVAILABILITY

All data are available from the authors.

## AUTHORS' CONTRIBUTIONS

**Gideon Adamu Shallangwa** and **Adamu Uzairu** conceived and designed the study. **Fabian Audu Ugbe** carried out the study and drafted the manuscript. **Ibrahim Abdulkadir** conducted the technical editing. All authors read and approved the final manuscript.

## REFERENCES

1. Mitra AK, Mawson AR. Neglected Tropical Diseases: Epidemiology and Global Burden. *Trop Med Infect Dis.* 2017;2(3):36. doi:10.3390/tropicalmed2030036
2. Bakowski MA, Shiroodi RK, Liu R, Olejniczak J, Yang B, Gagaring K, et al. Discovery of short-course antiwobachial quinazolines for elimination of filarial worm infections. *Sci Transl Med.* 2019;11(491): eaav3523. doi:10.1126/scitranslmed.aav3523
3. Jacobs RT, Lunde CS, Freund YR, Hernandez V, Li X, Xia Y, et al. Boron-pleuromutilins as anti-wolbachia agents with potential for treatment of onchocerciasis and lymphatic filariasis. *J Med Chem.* 2019;62:2521–40. doi:10.1021/acs.jmedchem.8b01854
4. Carter DS, Jacobs RT, Freund Y, Berry P, Akama T, Easom EE, et al. Macrofilaricidal benzimidazole-benzoxaborole hybrids as an approach to the treatment of river blindness, part 2: ketone linked analogs. *ACS Infect Dis.* 2020;6(2):180-5. doi:10.1021/acsinfecdis.9b00397

5. Weil GJ, Bogus J, Christian M, Dubray C, Djuardi Y, Fischer PU, et al. The safety of double- and triple-drug community mass drug administration for lymphatic filariasis: A multicenter, open-label, cluster-randomized study. *PLoS Med.* 2019;16(6):e1002839. doi:10.1371/journal.pmed.1002839
6. Sashidhara KV, Rao KB, Kushwaha V, Modukuri RK, Verma R, Murthy PK. Synthesis and antifilarial activity of chalcone-thiazole derivatives against a human lymphatic filarial parasite, *Brugia malayi*. *Eur J Med Chem.* 2014;81:473-80. doi:10.1016/j.ejmech.2014.05.029
7. Slatko BE, Taylor MJ, Foster JM. The wolbachia endosymbiont as an anti-filarial nematode target. *Symbiosis.* 2010;51(1):55-65. doi:10.1007/s13199-010-0067-1
8. Bouchery T, Lefoulon E, Karadjian G, Nieguitsila A, Martin C. The symbiotic role of wolbachia in onchocercidae and its impact on filariasis. *Clin Microbiol Infect.* 2013;19(2):131-40. doi:10.1111/1469-0691.12069
9. Bakowski MA, McNamara CW. Advances in Antiwolbachial Drug Discovery for Treatment of Parasitic Filarial Worm Infections. *Trop Med Infect Dis.* 2019;4(3):108. doi:10.3390/tropicalmed4030108
10. Sulaiman WAW, Kamtchum-Tatuene J, Mohamed MH, Ramachandran V, Ching SM, Lim SMS, et al. Anti-Wolbachia therapy for onchocerciasis & lymphatic filariasis: Current perspectives. *Indian J Med Res.* 2019;149(6):706-14. doi:10.4103/ijmr.ijmr\_454\_17
11. Newman DJ, Cragg GM. 2.19 - Natural Products of Therapeutic Importance. *Compr Nat Prod II.* 2010;2:623-50. doi:10.1016/B978-008045382-8.00055-1
12. Dasenaki ME, Thomaidis, NS. Chapter 18 - Meat Safety: II Residues and Contaminants. *Lawrie's Meat Sci.* 2017;553-83. doi:10.1016/B978-0-08-100694-8.00018-2
13. Brown P, Dawson MJ. Chapter Three - A Perspective on the Next Generation of Antibacterial Agents Derived by Manipulation of Natural Products. *Prog Med Chem.* 2015;54:135-84. doi:10.1016/bs.pmch.2014.10.001
14. Paukner S, Riedl R. Pleuromutilins: Potent Drugs for Resistant Bugs-Mode of Action and Resistance. *Cold Spring Harb Perspect Med.* 2017;7(1):a027110. doi:10.1101/cshperspect.a027110
15. Novak R, Shlaes DM. The pleuromutilin antibiotics: a new class for human use. *Curr Opin Investig Drugs.* 2010;11(2):182-91.
16. Adeniji SE, Arthur DE, Abdullahi M, Abdullahi A, Ugbe FA. Computer-aided modeling of triazole analogues, docking studies of the compounds on DNA Gyrase enzyme and design of new hypothetical compounds with efficient activities. *J Biomol Struct Dyn.* 2020;40(9):4004-20. doi:10.1080/07391102.2020.1852963
17. Ibrahim MT, Uzairu A, Shallangwa GA, Uba S. Lead identification of some anti-cancer agents with prominent activity against Non-Small Cell Lung Cancer (NSCLC) and structure-based design. *Chem Afr.* 2020;3:1023-44. doi:10.1007/s42250-020-00191-y
18. Lawal HA, Uzairu A, Uba S. QSAR, molecular docking studies, ligand-based design and pharmacokinetic analysis on Maternal Embryonic Leucine Zipper Kinase (MELK) inhibitors as potential anti-triple-negative breast cancer (MDA-MB-231 cell line) drug compounds. *Bull Natl Res Cent.* 2021;45:90. doi:10.1186/s42269-021-00541-x
19. Ibrahim MT, Uzairu A, Uba S, Shallangwa GA. Design of more potent quinazoline derivatives as EGFRWT inhibitors for the treatment of NSCLC: A computational approach. *Future J Pharm Sci.* 2021;7:140. doi:10.1186/s43094-021-00279-3
20. Lipinski CA, Lombardo F, Dominy BW, Feeney PJ. Experimental and computational approaches to estimate solubility and permeability in drug discovery and development settings. *Adv Drug Deliv Rev.* 2001;46(1-3):3-26. doi:10.1016/S0169-409X(00)00129-0

21. Edache EI, Uzairu A, Mamza PA, Shallangwa GA. Computational modeling and analysis of the theoretical structure of thiazolino 2 pyridone amide inhibitors for *Yersinia pseudo-tuberculosis* and *Chlamydia trachomatis* Infectivity. *Bull Sci Res.* 2022;4(1):14-39. doi:[10.54392/bsr2212](https://doi.org/10.54392/bsr2212)
22. Lu L, Hu H, Hou H, Wang B. An improved B3LYP method in the calculation of organic thermochemistry and reactivity. *Comput Theor Chem.* 2013;1015:64-71. doi:[10.1016/j.comptc.2013.04.009](https://doi.org/10.1016/j.comptc.2013.04.009)
23. Li Z, Wan H, Shi Y, Ouyang P. Personal experience with four kinds of chemical structure drawing software: review on ChemDraw, ChemWindow, ISIS/Draw, and ChemSketch. *J Chem Inf Comput Sci.* 2004;44(5):1886-90. doi:[10.1021/ci049794h](https://doi.org/10.1021/ci049794h)
24. Ugbe FA, Shallangwa GA, Uzairu A, Abdulkadir I. Theoretical activity prediction, structure-based design, molecular docking and pharmacokinetic studies of some maleimides against *Leishmania donovani* for the treatment of leishmaniasis. *Bull Natl Res Cent.* 2022;46:92. doi:[10.1186/s42269-022-00779-z](https://doi.org/10.1186/s42269-022-00779-z)
25. Hsu K, Chen Y, Lin S, Yang J. iGEMDOCK: a graphical environment of enhancing GEMDOCK using pharmacological interactions and post-screening analysis. *BMC Bioinform.* 2011;12(Suppl 1):S33. doi:[10.1186/1471-2105-12-S1-S33](https://doi.org/10.1186/1471-2105-12-S1-S33)
26. Ugbe FA, Shallangwa GA, Uzairu A, Abdulkadir I. Activity modeling, molecular docking and pharmacokinetic studies of some boron-pleuromutilins as anti-wolbachia agents with potential for treatment of filarial diseases. *Chem Data Collect.* 2021;36:100783. doi:[10.1016/j.cdc.2021.100783](https://doi.org/10.1016/j.cdc.2021.100783)
27. Du X, Li Y, Xia YL, Ai SM, Liang J, Sang P, et al. Insights into Protein-Ligand Interactions: Mechanisms, Models, and Methods. *Int J Mol Sci.* 2016;17(2):144. doi:[10.3390/ijms17020144](https://doi.org/10.3390/ijms17020144)
28. Sun Y, Yang AW, Hung A, Lenon GB. Screening for a potential therapeutic agent from the herbal formula in the 4<sup>th</sup> edition of the Chinese national guidelines for the initial-stage management of COVID-19 via molecular docking. *Evid Based Complement Alternat Med.* 2020;2020:3219840. doi:[10.1155/2020/3219840](https://doi.org/10.1155/2020/3219840)
29. Lee J, Cheng X, Swails JM, Yeom MS, Eastman PK, Lemkul JA, et al. CHARMM-GUI input generator for NAMD, GROMACS, AMBER, OpenMM, and CHARMM/OpenMM simulations using the CHARMM36 additive force field. *J Chem Theory Comput.* 2016;12(1):405-13. doi:[10.1021/acs.jctc.5b00935](https://doi.org/10.1021/acs.jctc.5b00935)
30. Phillips JC, Braun R, Wang W, Gumbart J, Tajkhorshid E, Villa E, et al. Scalable molecular dynamics with NAMD. *J Comput Chem.* 2005;26(16):1781-802. doi:[10.1002/jcc.20289](https://doi.org/10.1002/jcc.20289)
31. Edache EI, Uzairu A, Mamza PA, Shallangwa GA. A comparative QSAR analysis, 3D-QSAR, molecular docking and molecular design of iminoguanidine-based inhibitors of HemO: A rational approach to antibacterial drug design. *J Drugs Pharm Sci.* 2020;4(3):21-36. doi:[10.31248/JDPS2020.036](https://doi.org/10.31248/JDPS2020.036)